Rapid Communications

Observation of persistent orientation of chiral molecules by a laser field with twisted polarization

Ilia Tutunnikov,[1] Johannes Floß,[2] Erez Gershnabel,[1] Paul Brumer,[2] Ilya Sh. Averbukh,[1,*]
Alexander A. Milner,[3] and Valery Milner[3,†]

[1]*AMOS and Department of Chemical and Biological Physics, The Weizmann Institute of Science, Rehovot 7610001, Israel*
[2]*Chemical Physics Theory Group, Department of Chemistry, and Center for Quantum Information and Quantum Control, University of Toronto, Toronto, Ontario, Canada M5S 3H6*
[3]*Department of Physics & Astronomy, The University of British Columbia, Vancouver, British Columbia, Canada V6T 1Z1*

(Received 16 October 2019; accepted 3 February 2020; published 24 February 2020)

Molecular chirality is an omnipresent phenomenon of fundamental significance in physics, chemistry, and biology. For this reason, the search for various techniques for enantioselective control, detection, and separation of chiral molecules is of particular importance. It has been recently predicted that laser fields with twisted polarization may induce a persistent enantioselective field-free orientation of chiral molecules. Here, we report an experimental observation of this phenomenon using propylene oxide molecules (CH_3CHCH_2O, or PPO) spun by an optical centrifuge—a laser pulse—whose linear polarization undergoes an accelerated rotation around its propagation direction. We show that PPO molecules remain oriented on a timescale exceeding the duration of the centrifuge pulse by several orders of magnitude. The demonstrated long-time field-free enantioselective orientation may open new avenues for optical manipulation, discrimination, and, potentially, the separation of molecular enantiomers.

DOI: 10.1103/PhysRevA.101.021403

Chiral molecules exist in two nonsuperimposable forms called enantiomers [1]. The ability to analyze and separate mixtures of enantiomers is crucial, for example, in drug synthesis as different enantiomers of chiral molecules may exhibit strikingly different biological activities. Over the years, various optical approaches have been developed to control molecules in the gas phase and induce their alignment and orientation (for recent reviews, see, e.g., Refs. [2–5]; the earlier developments are reviewed in Ref. [6]). The most known technique of this kind is the field-free *alignment* of linear molecules by short linearly polarized laser pulses, which kicks the most polarizable molecular axis towards the line defined by the pulse polarization (see Refs. [2–6]; see also Ref. [7] and references therein). Laser-induced molecular *orientation* is a more challenging task; nevertheless, several techniques have been suggested and demonstrated for the impulsive orientation of linear and even asymmetric top molecules under field-free conditions (for recent reviews, see Refs. [4,5]; see also Ref. [8] and references therein).

Owing to the symmetry of light interaction with the induced dipole moment, strong laser fields with a fixed linear polarization can be utilized only to align, but not to orient, molecules in space. In contrast, fields with twisting polarization break this symmetry, and were predicted to transiently orient chiral molecules [9–11], as was recently confirmed experimentally [12].

Here, we report an observation of a remarkable phenomenon predicted theoretically in Refs. [10,11,13]—field-free *persistent* enantioselective orientation (PESO) of chiral molecules, which lasts orders of magnitude longer than the duration of the excitation laser pulses. The effect appears when chiral molecules are driven by pulsed nonresonant laser fields with twisted polarization. The simplest example of such a field is a pair of delayed cross-polarized laser pulses [14,15], and there is plethora of more sophisticated examples, including chiral pulse trains [16–18], polarization-shaped pulses [19–21], and an optical centrifuge [22–26].

In all the previously known approaches to impulsive molecular orientation, including techniques using single-cycle THz pulses [27–33], alone or in combination with optical pulses [34–36], or two-color laser fields [8,28,37–43], the orientation is short lived and disappears rapidly after the end of the excitation pulses. Transient revival spikes may appear at longer times, however, they ride on a zero baseline and their time average is exactly zero.

Here, we observe an anomalously long-lasting enantioselective orientation, having a nonzero baseline persisting on timescales exceeding the duration of the excitation pulse by several orders of magnitude, in full agreement with the theoretical expectations [10,11,13].

In what follows, we begin with a qualitative discussion of the PESO phenomenon, then present its experimental observation using chiral propylene oxide molecules spun by an optical centrifuge. Finally, we present the results of the quantum simulation of the PESO phenomenon. The results of the experimental measurements are in a good agreement with the theoretical predictions.

Qualitative discussion. This section briefly discusses the origin of the PESO phenomenon (a more detailed discussion can be found in our extended theoretical work [13]). To be specific, we use a particular example of propylene oxide molecule (CH_3CHCH_2O, or PPO) excited by an optical

*ilya.averbukh@weizmann.ac.il
†vmilner@phas.ubc.ca

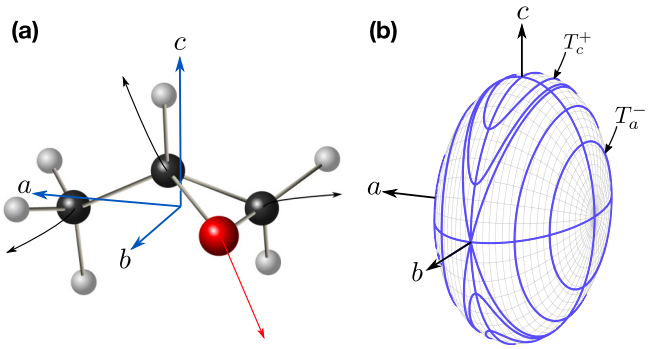

FIG. 1. (a) (*R*)-propylene oxide molecule. Atoms are color coded: black, carbon; light gray, hydrogen; red (dark gray), oxygen. Principal axes of inertia tensor ($\mathcal{I}$ frame) are shown as solid arrows and labeled by a, b, and c (moments of inertia are ordered $I_a < I_b < I_c$). Coulomb explosion trajectories from a stationary molecule are shown with thin lines (see Experimental Methods section for details). (b) Binet ellipsoid. Shown in blue (thick) lines are the allowed trajectories of the angular momentum vector. As an example, two trajectories (T_a^- and T_c^+) are labeled according to the notation used in text.

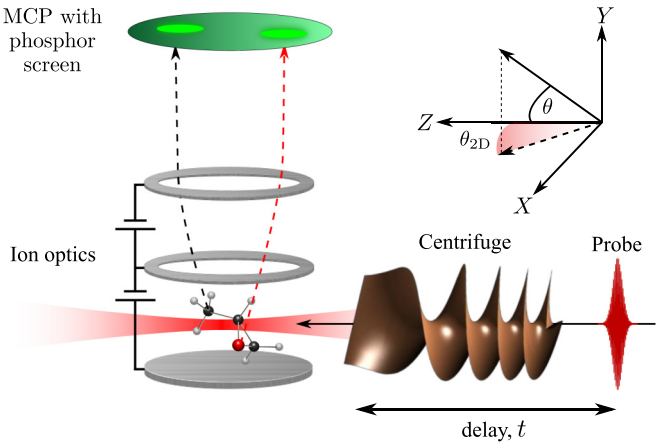

FIG. 2. Schematic illustration of our experimental geometry. Cold PPO molecules in a seeded helium jet are spun in an optical centrifuge and Coulomb exploded with a probe pulse between the plates of a conventional velocity map imaging spectrometer, equipped with a multichannel plate (MCP) detector and a phosphor screen. The inset shows the fixed frame axes and the definition of angles θ and θ_{2D} used in text. Coulomb explosion trajectories from a stationary molecule are shown with thin lines in Fig. 1(a).

centrifuge [22–24,44]. Figure 1(a) shows one of the enantiomers of PPO [right handed, (*R*)-PPO] with its principal axes of the moment of inertia (a, b, and c). At the classical level, the trajectories followed by the angular momentum vector $\mathbf{L}$ in the frame of principal axes are defined by the intersection of an ellipsoid with semiaxes $\sqrt{2EI_a}$, $\sqrt{2EI_b}$, and $\sqrt{2EI_c}$, and a sphere of radius L,

$$\frac{L_a^2}{2EI_a}+\frac{L_b^2}{2EI_b}+\frac{L_c^2}{2EI_c}=1, \qquad \frac{L_a^2+L_b^2+L_c^2}{L^2}=1, \tag{1}$$

where I_j are the moments of inertia, L_j are the components of the angular momentum vector ($j=a,b,c$) whose magnitude is L, and E is the rotational energy. The moments of inertia are ordered as $I_a < I_b < I_c$. The trajectories can be visualized with the help of Binet construction [45] [see Fig. 1(b)]. The trajectories enclosing the poles of the a and c axes are denoted by $T_k^{\pm}$ ($k=a,c$), where $\pm$ refers to the positive/negative side of the axis [see Fig. 1(b)]. On these trajectories, the sign of L_k is conserved and it matches the sign of the trajectory label ($T_k^{\pm}$). This means that in the course of a free rotation of individual asymmetric top molecules, their a and c axes on average point either along or against the angular momentum vector, but never flip their direction.

It is possible to optically excite an initially isotropic ensemble of chiral molecules in such a way that the ensemble-averaged quantities $\langle \hat{\mathbf{a}}\cdot\hat{\mathbf{Z}}\rangle$ or $\langle \hat{\mathbf{c}}\cdot\hat{\mathbf{Z}}\rangle$ (here, Z is some axis in the laboratory frame) keep their sign unchanged with time as well. This can be achieved by a combination of two processes: first, by orienting the averaged angular momentum vector along this axis, and, second, by breaking the T_k^+ vs T_k^- symmetry.

Fields with twisted polarization in general, and the field of an optical centrifuge in particular, can satisfy both requirements when acting upon chiral molecules. An optical centrifuge orients the averaged angular momentum vector perpendicular to the plane of twisting. Also, it induces a torque (depending on the off-diagonal elements of polarizability) which orients the molecules themselves perpendicular to the plane [10,11]. In addition, it can be shown that this torque also breaks the T_k^+ vs T_k^- symmetry, allowing the long-term orientation [13].

The persistence of the signs of $\langle \hat{\mathbf{a}}\cdot\hat{\mathbf{Z}}\rangle$ and/or $\langle \hat{\mathbf{c}}\cdot\hat{\mathbf{Z}}\rangle$ implies that for any vector $\mathbf{v}$ fixed in the $\mathcal{I}$ frame, the quantity $\langle \hat{\mathbf{v}}\cdot\hat{\mathbf{Z}}\rangle$ has a constant sign, too. This is important for our experiments, utilizing the Coulomb explosion technique, because for chiral molecules fragment trajectories do not usually coincide with the directions defined by the molecular axes $\mathbf{a}$ and $\mathbf{c}$.

Experimental methods and results. Our setup for producing the field of an optical centrifuge has been built according to the original recipe of Karzmarek *et al.* [22] and was described in an earlier publication [44]. Briefly, we split the spectrum of broadband laser pulses from a Ti:sapphire amplifier (10 mJ, 35 fs, repetition rate 1 kHz, central wavelength 795 nm) in two equal parts using a Fourier pulse shaper. The two beams are first frequency chirped with a chirp rate β of equal magnitude and opposite sign ($\beta=\pm 0.3$ rad ps^{-2}). The chirped beams are then circularly polarized with an opposite sense of circular polarization. The optical interference of these laser fields results in a pulse illustrated in Fig. 2: Its polarization vector is rotating in the XY plane with an instantaneous angular frequency $\Omega=2\beta t$. The effect of imperfect circular polarization was thoroughly studied with the help of simulations, and it was found to have no effect on the main results presented below. The duration of our centrifuge pulse is 20 ps.

We use a typical velocity map imaging (VMI) setup [46] in which the molecular jet is intercepted by an intense femtosecond probe beam between the plates of a time-of-flight (TOF) spectrometer (see Fig. 2). Multiple ionization of a molecule by the probe beam [full width at half maximum (FWHM) 50 fs, 10^{15} W/cm^2] results in a Coulomb explosion, i.e., breaking

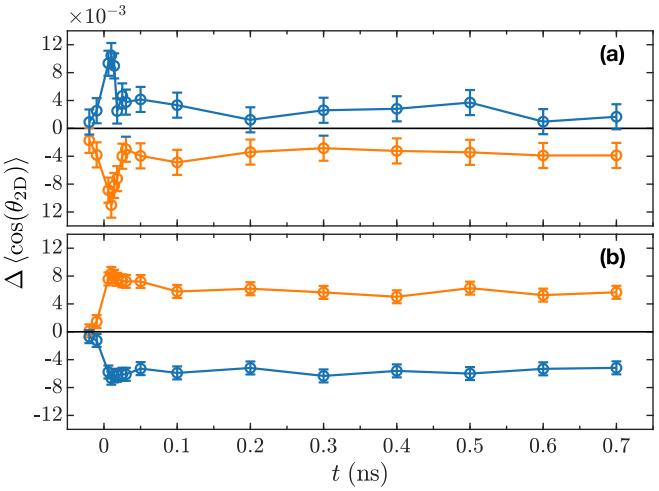

FIG. 3. Experimentally measured two-dimensional (2D) orientation factor $\Delta\langle\cos(\theta_{2D})\rangle$ in the velocity distribution of (a) O^+ and (b) C^+ fragments as a function of optical centrifuge-probe pulse delay t. Orange (light gray): right-handed molecule, (R)-PPO; blue (dark gray): left-handed molecule, (S)-PPO. Note the reversal of colors between the two plots.

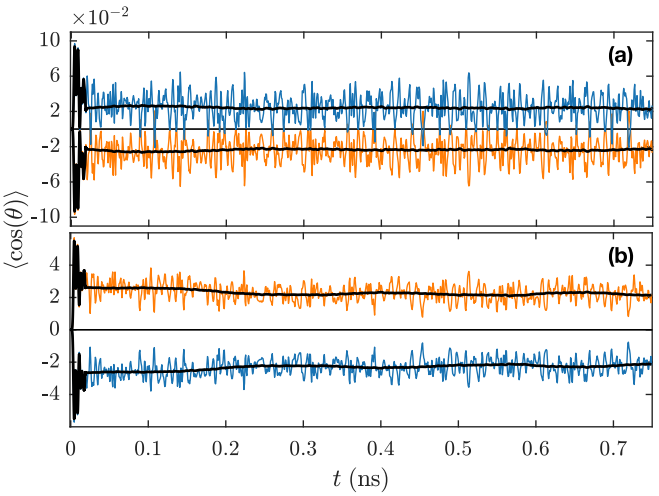

FIG. 4. Results of quantum mechanical calculations, showing the expectation value of the 3D orientation factor $\langle\cos(\theta)\rangle$ where θ is the angle between the ions' velocity vector and Z axis [see Fig. 2] for (a) the oxygen ion velocity vector and (b) the carbon ion velocity (averaged over the three carbons). See the main text for the description of the calculation of the ion's velocities. Orange (light gray): (R)-PPO; blue (dark gray): (S)-PPO. The solid black curves present the sliding time window averages of the signal, $\overline{\langle\cos(\theta)\rangle}(t) = (\Delta t)^{-1}\int_{t-\Delta t/2}^{t+\Delta t/2}\langle\cos(\theta)\rangle(t')dt'$, where $\Delta t = 100$ ps. The parameters of the optical centrifuge pulse are peak intensity $I_0 = 5\times10^{12}$ W/cm^2, $\beta = 0.05$ rad ps^{-2}, duration $t_p = 20$ ps. The initial rotational temperature was set to $T = 0$ K.

of the molecule into ionized fragments. As the fragment ions accelerate towards, and impinge on, the multichannel plate detector (MCP), the projection of their velocities on the XZ plane is mapped on the plane of the detector.

The VMI dc field strength in our setup was ≈800 V/cm, with an estimated component along the orientation direction at least two orders of magnitude weaker than that required for the mixed-field orientation [47,48]. Mass selectivity is provided by gating the MCP at the time of arrival of the fragment of interest. According to our experimental analysis (covariance TOF), at this ionization regime the PPO molecule breaks mostly into singly and doubly ionized atomic fragments. Larger polyatomic fragments (specifically, OCH_2^+ and $C_2H_4^+$) are typically seen at lower intensities but are not accompanied by C^+ and O^+ fragments. The time constants of our MCP gate (20 ns) and of a phosphor screen (<10 ns) lead to a mass resolution of 1 amu. A simplified model of the Coulomb explosion shown in Fig. 1(a) predicts that the velocities of C^+ ions (averaged over three carbon atoms) and O^+ ions have opposite projections on the laboratory Z axis (see Fig. 4), in full qualitative agreement with the experimental observations (see Fig. 3).

We extract the information about the molecular orientation in the laboratory frame as a function of time by recording VMI images at different centrifuge-probe time delays (see Fig. 2). The experimental observable, bearing the information about the degree of orientation, is conventionally determined as $\langle\cos(\theta_{2D})\rangle$. Here, θ_{2D} is the angle between the projection of the fragment's velocity $\mathbf{v}$ on the velocity map imaging detector plane (XZ plane) and the laboratory Z axis, where $\langle\cdots\rangle$ implies averaging over the molecular ensemble. Positive (negative) values of $\langle\cos(\theta_{2D})\rangle$ reflect the orientation of $\mathbf{v}$ along (against) the laboratory Z axis. In practice, an average of a few million ion fragments were recorded for each set of experimental conditions, resulting in a precision of 10^{-3} in determining $\langle\cos(\theta_{2D})\rangle$. Approximately 20 ions per 10 laser shots (the duration of a single VMI frame) were recorded on average. To minimize systematic errors, e.g., due to the inhomogeneous response of our detector as well as long-term drifts in molecular density and laser intensity, we define the following quantity (hereafter referred to as the "2D orientation factor"),

$$\begin{aligned}\Delta\langle\cos(\theta_{2D})\rangle &\equiv \langle\cos(\theta_{2D})\rangle_{\circlearrowright} - \langle\cos(\theta_{2D})\rangle_{\circlearrowleft}\\ &= \pm 2\langle\cos(\theta_{2D})\rangle_{\circlearrowright,\circlearrowleft},\end{aligned}$$

where the indices $\circlearrowright$ and $\circlearrowleft$ correspond to the clockwise and counterclockwise direction of polarization rotation, as observed along the laser beam propagation.

In Fig. 3 we plot the experimentally measured $\Delta\langle\cos(\theta_{2D})\rangle$ for the velocity distributions of O^+ and C^+ fragments. For both, the enantioselective effect of the centrifuge is reflected by the opposite sign of the 2D orientation factor $\Delta\langle\cos(\theta_{2D})\rangle$ for the two enantiomers. In the case of oxygen ions [Fig. 3(a)], $|\Delta\langle\cos(\theta_{2D})\rangle|$ reaches values of the order of 10^{-2} during the interaction with the centrifuge field (first 20 ps), being positive for left- and negative for right-handed molecules. When the interaction is over, the degree of orientation becomes smaller, but maintains a nonzero value of opposite signs for at least 700 ps (a maximum accessible delay time in the current experimental setup). Carbon ions demonstrate similar behavior, shown in Fig. 3(b). The nonzero 2D orientation factor $\Delta\langle\cos(\theta_{2D})\rangle$ of C^+ also persists on the full available timescale. As seen, the orientation signals of O^+ and C^+ ions are opposite to each other for both enantiomers, in agreement with theoretical simulations (see Fig. 4).

Theoretical results. The chiral molecule is modeled as a rigid asymmetric top having anisotropic polarizability. We carry out both classical and fully quantum simulations of the rotational dynamics. The molecular parameters and details of our theoretical approaches may be found in Refs. [11,13].

We adopted a simplified model of a Coulomb explosion, which assumes an instantaneous conversion of all constituent atoms into singly charged ions, while keeping the molecular configuration unchanged during the interaction with the probe pulse [12]. Trajectories of the fragments are shown in Fig. 1(a) by red and black arrowed lines for oxygen and carbon ions, respectively. A static PPO molecule would eject its ions along these directions that carry the information about the spatial orientation of the molecule at the moment of explosion.

In the current experiment, the estimated rotational temperature of the molecules is 10 K, the same as in our recent experiment [12]. The theoretical analysis in Ref. [12] fully took into account the temperature effects. Here, however, we limited our simulations to $T = 0$ K, which provides orientation values comparable to that of $T = 10$ K [13] (see Fig. 7 there), thus allowing us to extend the simulated time period by several orders of magnitude.

Figure 4 shows the results of our quantum mechanical simulations, and presents the conventional (3D) orientation factors $\langle\cos(\theta)\rangle$—the expectation values of the projection of the oxygen and carbon ions' velocity vectors on the laser propagation direction (Z axis in Fig. 2). Here, θ is the angle between the velocity vector and Z axis, and $\langle\cdots\rangle$ denotes the ensemble average or quantum expectation value for the classical and quantum mechanical simulations, respectively. The presented orientation factor $\langle\cos(\theta)\rangle$ for the carbon ions was obtained by averaging the results for the three individual molecular carbons. Despite the simplicity of the adopted Coulomb explosion model, there is a full correlation between the distinctive features of the simulated and the experimentally measured signals: (1) Both of them are enantioselective, i.e., opposite for the two enantiomers; (2) simulated signals reproduce the observed persistency of the orientation; and (3) the theoretical model predicts the experimentally observed opposite signs of the $\langle\cos(\theta)\rangle$ values for the C^+ and O^+ ions velocities. The orientation within our observation window (20–700 ps) is practically permanent, and opposite for the two enantiomers. For additional details, we refer the reader to our previous publications [12,13].

During the operation of the optical centrifuge, the angular momentum increases. Figures 5(a) and 5(b) show the distribution of the angular momentum magnitude (in units of $\hbar$) as a function of time during the optical centrifuge operation (20 ps). It is evident that the molecules undergo a forced angular acceleration. Figure 5(c) shows the simulated (both classically and quantum mechanically) 3D orientation factors $\langle\cos(\theta)\rangle$ for the corresponding time. The solid black curve represents the envelope of the optical centrifuge field showing that the peak intensity is reached after 2 ps.

For computational reasons, the angular acceleration used in our simulation is lower than the experimental one (by a factor of 6). The maximum attainable magnitude of the angular momentum $J_{\max}$ is proportional to the product $t_p\beta$, while the basis size required for full quantum simulations of the asymmetric-top molecule scales as $J_{\max}^3$. The cubic scaling

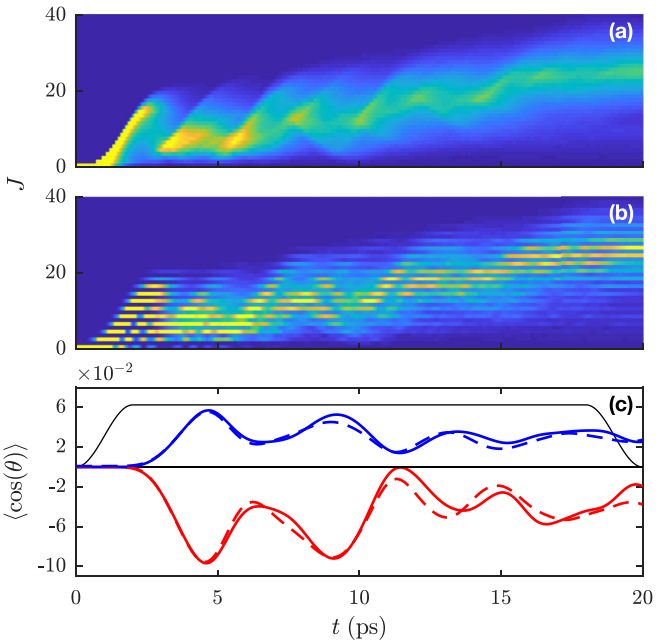

FIG. 5. Distribution of the angular momentum in units of $\hbar$, J as a function of time calculated (a) classically and (b) quantum mechanically. (c) Short-time dynamics of the 3D orientation factors of (R)-PPO, $\langle\cos(\theta)\rangle$. The angle θ is the angle between the ion's velocity vector and Z axis [see Fig. 2]. The solid blue (dark gray) and red (light gray) curves are results of quantum mechanical simulations for the carbon and oxygen ions' velocities, respectively, whereas the dashed lines show the results of classical simulations for comparison. The solid black curve represents the intensity profile of the optical centrifuge field in arbitrary units. The parameters of the optical centrifuge are the same as in Fig. 4.

forbids the direct quantum calculation involving very high angular momentum states, although some progress is offered by the semiclassical methods [49]. Moreover, at high J values, the rigid-top approximation becomes invalid. However, even with the chosen β value, our simulations qualitatively reproduce the observed effect.

In Ref. [13], it was pointed out that quantum effects lead to degradation of the orientation on the long-time scale, while this orientation is indefinitely permanent in the classical model. To illustrate a smooth transition of the quantum orientation dynamics into the one predicted by the classical theory, we discuss the quantum mechanical behavior of our system for various degrees of rotational excitation.

One of the ways to control the degree of rotational excitation is by changing the duration of the centrifuge pulse t_p. Figure 6 focuses on the simulated orientation of the oxygen ion velocity vector $\langle\cos\theta\rangle$ within the experimentally accessible time window, but for various durations of the centrifuge pulse t_p. As may be seen from Fig. 6(a), a relativity short centrifuge of $t_p = 10$ ps (providing a relatively low degree of rotational excitation with a mean value of angular momentum $\langle J\rangle \approx 12$) results in high-frequency quantum beats riding on a slowly oscillating coarse-grained time average (over a sliding time window of $\Delta t = 100$ ps; see the solid and dashed black curves). This is a behavior expected for a rotational wave

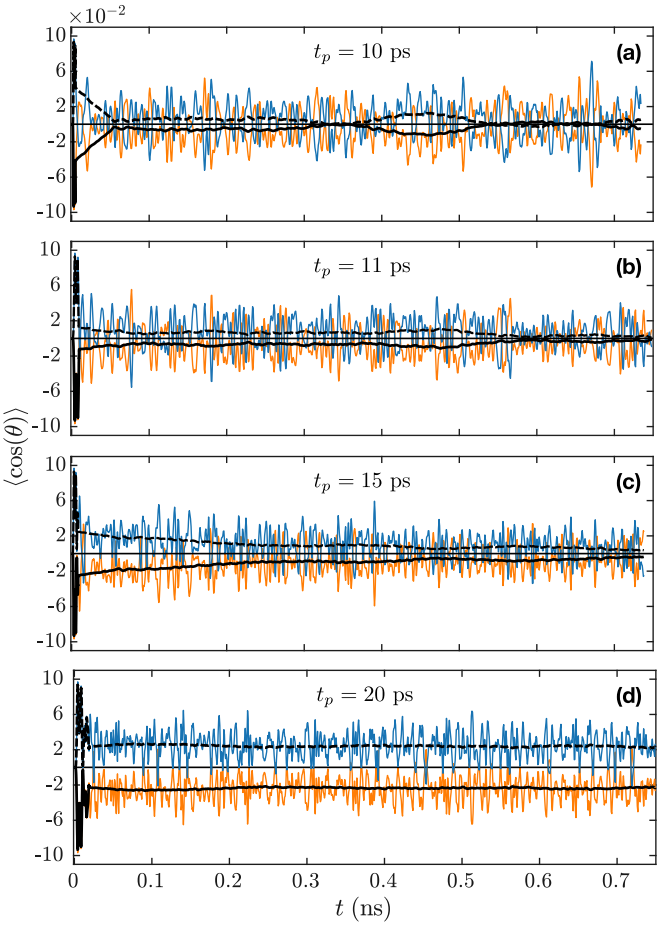

FIG. 6. Results of quantum mechanical calculations, showing $\langle\cos(\theta)\rangle$ of the oxygen ion velocity for increasing rotational excitation starting from (a) a mean angular momentum $\langle J\rangle = 12$ up to (d) $\langle J\rangle = 24$. Orange (light gray): (*R*)-PPO; blue (dark gray): (*S*)-PPO. The solid and dashed black curves present sliding time window averages as in Fig. 4. All the parameters are similar to Fig. 4, while (a) $t_p = 10$ ps, (b) $t_p = 11$ ps, (c) $t_p = 15$ ps, and (d) $t_p = 20$ ps [similar to Fig. 4(a)].

packet consisting of a relatively small number of angular momentum states. When the duration of the centrifuge is slightly increased to $t_p = 11$ ps [Fig. 6(b)], a nonzero baseline appears for the above-mentioned coarse-grained signals, which have opposite signs for the two enantiomers of the PPO molecule. The oscillatory behavior is pushed to longer times. In the case of $t_p = 15$ ps [Fig. 6(c)], the coarse-grained oscillations are pushed even further, and are not observed within the experimental time window (≈750 ps).

Finally, for $t_p = 20$ ps (corresponding to the actual duration of the optical centrifuge pulse in our experiments), the two orientation baselines are practically constant within the 750 ps time window [see Fig. 6(d)].

Conclusions. Following the theoretical prediction of Ref. [13], we experimentally demonstrated the phenomenon of persistent enantioselective orientation (PESO) of chiral molecules excited by laser fields with twisted polarization. We found very good qualitative agreement between the quantum mechanical simulations and the experimental results. The molecular orientation direction depends on both the sense of polarization twisting and the handedness of the molecule. A higher degree of orientation is expected at lower temperatures of the gas, as shown in Fig. 4, where an orientation degree of ≈3% is predicted at 0 K. The effect of angular acceleration of the centrifuge on $\langle\cos(\theta)\rangle$ was outside of the scope of our work, and needs to be carefully analyzed in terms of its influence on the chiral selectivity. Similarly, using bichromatic fields, elliptical polarization, and/or dc external fields may offer other ways of enhancing the observed effect.

This long-lasting orientation, unavailable in previous schemes of orienting molecules with electromagnetic fields, provides modalities for controlling the motion of chiral molecules, detecting molecular chirality by means of nonlinear optics, and potentially for separating the laser-oriented enantiomers in external inhomogeneous fields (see, e.g., Refs. [48,50,51], references therein, and recent reviews [3,4,52]).

Acknowledgments. This work was supported by the Israel Science Foundation (Grant No. 746/15), the ISF-NSFC joint research program (Grant No. 2520/17), and by Natural Sciences and Engineering Research Council of Canada grants to P.B. and to V.M. The work of A.A.M. and V.M. was carried out under the auspices of the Canadian Center for Chirality Research on Origins and Separation (CHIROS), funded by Canada Foundation for Innovation. I.A. acknowledges support as the Patricia Elman Bildner Professorial Chair, and thanks the UBC Department of Physics & Astronomy for hospitality extended to him during his sabbatical stay. This research was made possible in part by the historic generosity of the Harold Perlman Family.

[1] F. A. Cotton, *Chemical Applications of Group Theory*, 3rd ed. (Wiley, Hoboken, NJ, 1990).

[2] Y. Ohshima and H. Hasegawa, Coherent rotational excitation by intense nonresonant laser fields, Int. Rev. Phys. Chem. **29**, 619 (2010).

[3] S. Fleischer, Y. Khodorkovsky, E. Gershnabel, Y. Prior, and I. Sh. Averbukh, Molecular alignment induced by ultrashort laser pulses and its impact on molecular motion, Isr. J. Chem. **52**, 414 (2012).

[4] M. Lemeshko, R. V. Krems, J. M. Doyle, and S. Kais, Manipulation of molecules with electromagnetic fields, Mol. Phys. **111**, 1648 (2013).

[5] C. P. Koch, M. Lemeshko, and D. Sugny, Quantum control of molecular rotation, Rev. Mod. Phys. **91**, 035005 (2019).

[6] H. Stapelfeldt and T. Seideman, Colloquium: Aligning molecules with strong laser pulses, Rev. Mod. Phys. **75**, 543 (2003).

[7] E. T. Karamatskos, S. Raabe, T. Mullins, A. Trabattoni, P. Stammer, G. Goldsztejn, R. R. Johansen, K. Długołecki, H. Stapelfeldt, M. J. J. Vrakking, S. Trippel, A. Rouzée, and J. Küpper, Molecular movie of ultrafast coherent rotational dynamics of OCS, Nat. Commun. **10**, 3364 (2019).

[8] K. Lin, I. Tutunnikov, J. Qiang, J. Ma, Q. Song, Q. Ji, W. Zhang, H. Li, F. Sun, X. Gong, H. Li, P. Lu, H. Zeng, Y. Prior, I. Sh. Averbukh, and J. Wu, All-optical field-free three-dimensional orientation of asymmetric-top molecules, Nat. Commun. **9**, 5134 (2018).

[9] A. Yachmenev and S. N. Yurchenko, Detecting Chirality in Molecules by Linearly Polarized Laser Fields, Phys. Rev. Lett. **117**, 033001 (2016).

[10] E. Gershnabel and I. Sh. Averbukh, Orienting Asymmetric Molecules by Laser Fields with Twisted Polarization, Phys. Rev. Lett. **120**, 083204 (2018).

[11] I. Tutunnikov, E. Gershnabel, S. Gold, and I. Sh. Averbukh, Selective orientation of chiral molecules by laser fields with twisted polarization, J. Phys. Chem. Lett **9**, 1105 (2018).

[12] A. A. Milner, J. A. M. Fordyce, I. MacPhail-Bartley, W. Wasserman, V. Milner, I. Tutunnikov, and I. Sh. Averbukh, Controlled Enantioselective Orientation of Chiral Molecules with an Optical Centrifuge, Phys. Rev. Lett. **122**, 223201 (2019).

[13] I. Tutunnikov, J. Floß, E. Gershnabel, P. Brumer, and I. Sh. Averbukh, Laser-induced persistent orientation of chiral molecules, Phys. Rev. A **100**, 043406 (2019).

[14] S. Fleischer, Y. Khodorkovsky, Y. Prior, and I. Sh. Averbukh, Controlling the sense of molecular rotation, New J. Phys. **11**, 105039 (2009).

[15] K. Kitano, H. Hasegawa, and Y. Ohshima, Ultrafast Angular Momentum Orientation by Linearly Polarized Laser Fields, Phys. Rev. Lett. **103**, 223002 (2009).

[16] S. Zhdanovich, A. A. Milner, C. Bloomquist, J. Floß, I. Sh. Averbukh, J. W. Hepburn, and V. Milner, Control of Molecular Rotation with a Chiral Train of Ultrashort Pulses, Phys. Rev. Lett. **107**, 243004 (2011).

[17] C. Bloomquist, S. Zhdanovich, A. A. Milner, and V. Milner, Directional spinning of molecules with sequences of femtosecond pulses, Phys. Rev. A **86**, 063413 (2012).

[18] J. Floß and I. Sh. Averbukh, Molecular spinning by a chiral train of short laser pulses, Phys. Rev. A **86**, 063414 (2012).

[19] G. Karras, M. Ndong, E. Hertz, D. Sugny, F. Billard, B. Lavorel, and O. Faucher, Polarization Shaping for Unidirectional Rotational Motion of Molecules, Phys. Rev. Lett. **114**, 103001 (2015).

[20] E. Prost, H. Zhang, E. Hertz, F. Billard, B. Lavorel, P. Bejot, J. Zyss, I. Sh. Averbukh, and O. Faucher, Third-order-harmonic generation in coherently spinning molecules, Phys. Rev. A **96**, 043418 (2017).

[21] E. Prost, E. Hertz, F. Billard, B. Lavorel, and O. Faucher, Polarization-based tachometer for measuring spinning rotors, Opt. Express **26**, 31839 (2018).

[22] J. Karczmarek, J. Wright, P. Corkum, and M. Ivanov, Optical Centrifuge for Molecules, Phys. Rev. Lett. **82**, 3420 (1999).

[23] D. M. Villeneuve, S. A. Aseyev, P. Dietrich, M. Spanner, M. Yu. Ivanov, and P. B. Corkum, Forced Molecular Rotation in an Optical Centrifuge, Phys. Rev. Lett. **85**, 542 (2000).

[24] L. Yuan, S. W. Teitelbaum, A. Robinson, and A. S. Mullin, Dynamics of molecules in extreme rotational states, Proc. Natl. Acad. Sci. USA **108**, 6872 (2011).

[25] A. Korobenko, A. A. Milner, and V. Milner, Direct Observation, Study, and Control of Molecular Superrotors, Phys. Rev. Lett. **112**, 113004 (2014).

[26] A. Korobenko, Control of molecular rotation with an optical centrifuge, J. Phys. B **51**, 203001 (2018).

[27] H. Harde, S. Keiding, and D. Grischkowsky, THz Commensurate Echoes: Periodic Rephasing of Molecular Transitions in Free-Induction Decay, Phys. Rev. Lett. **66**, 1834 (1991).

[28] C. M. Dion, A. D. Bandrauk, O. Atabek, A. Keller, H. Umeda, and Y. Fujimura, Two-frequency IR laser orientation of polar molecules. Numerical simulations for HCN, Chem. Phys. Lett. **302**, 215 (1999).

[29] I. Sh. Averbukh and R. Arvieu, Angular Focusing, Squeezing, and Rainbow Formation in a Strongly Driven Quantum Rotor, Phys. Rev. Lett. **87**, 163601 (2001).

[30] M. Machholm and N. E. Henriksen, Field-Free Orientation of Molecules, Phys. Rev. Lett. **87**, 193001 (2001).

[31] S. Fleischer, Y. Zhou, R. W. Field, and K. A. Nelson, Molecular Orientation and Alignment by Intense Single-Cycle THz Pulses, Phys. Rev. Lett. **107**, 163603 (2011).

[32] K. Kitano, N. Ishii, N. Kanda, Y. Matsumoto, T. Kanai, M. Kuwata-Gonokami, and J. Itatani, Orientation of jet-cooled polar molecules with an intense single-cycle THz pulse, Phys. Rev. A **88**, 061405 (2013).

[33] R. Damari, S. Kallush, and S. Fleischer, Rotational Control of Asymmetric Molecules: Dipole- Versus Polarizability-Driven Rotational Dynamics, Phys. Rev. Lett. **117**, 103001 (2016).

[34] D. Daems, S. Guérin, D. Sugny, and H. R. Jauslin, Efficient and Long-Lived Field-Free Orientation of Molecules by a Single Hybrid Short Pulse, Phys. Rev. Lett. **94**, 153003 (2005).

[35] E. Gershnabel, I. Sh. Averbukh, and R. J. Gordon, Orientation of molecules via laser-induced antialignment, Phys. Rev. A **73**, 061401 (2006).

[36] K. N. Egodapitiya, S. Li, and R. R. Jones, Terahertz-Induced Field-Free Orientation of Rotationally Excited Molecules, Phys. Rev. Lett. **112**, 103002 (2014).

[37] M. J. J. Vrakking and S. Stolte, Coherent control of molecular orientation, Chem. Phys. Lett. **271**, 209 (1997).

[38] T. Kanai and H. Sakai, Numerical simulations of molecular orientation using strong, nonresonant, two-color laser fields, J. Chem. Phys **115**, 5492 (2001).

[39] S. De, I. Znakovskaya, D. Ray, F. Anis, Nora G. Johnson, I. A. Bocharova, M. Magrakvelidze, B. D. Esry, C. L. Cocke, I. V. Litvinyuk, and M. F. Kling, Field-Free Orientation of CO Molecules by Femtosecond Two-Color Laser Fields, Phys. Rev. Lett. **103**, 153002 (2009).

[40] K. Oda, M. Hita, S. Minemoto, and H. Sakai, All-Optical Molecular Orientation, Phys. Rev. Lett. **104**, 213901 (2010).

[41] J. Wu and H. Zeng, Field-free molecular orientation control by two ultrashort dual-color laser pulses, Phys. Rev. A **81**, 053401 (2010).

[42] E. Frumker, C. T. Hebeisen, N. Kajumba, J. B. Bertrand, H. J. Wörner, M. Spanner, D. M. Villeneuve, A. Naumov, and P. B.

Corkum, Oriented Rotational Wave-Packet Dynamics Studies via High Harmonic Generation, Phys. Rev. Lett. **109**, 113901 (2012).

[43] N. Takemoto and K. Yamanouchi, Fixing chiral molecules in space by intense two-color phase-locked laser fields, Chem. Phys. Lett. **451**, 1 (2008).

[44] A. Korobenko, A. A. Milner, J. W. Hepburn, and V. Milner, Rotational spectroscopy with an optical centrifuge, Phys. Chem. Chem. Phys. **16**, 4071 (2014).

[45] H. Goldstein, *Classical Mechanics* (Addison-Wesley, San Francisco, 2002).

[46] A. T. J. B. Eppink and D. H. Parker, Velocity map imaging of ions and electrons using electrostatic lenses: Application in photoelectron and photofragment ion imaging of molecular oxygen, Rev. Sci. Instrum. **68**, 3477 (1997).

[47] S. Trippel, T. Mullins, N. L. M. Müller, J. S. Kienitz, R. González-Férez, and J. Küpper, Two-State Wave Packet for Strong Field-Free Molecular Orientation, Phys. Rev. Lett. **114**, 103003 (2015).

[48] A. Yachmenev, J. Onvlee, E. Zak, A. Owens, and J. Küpper, Field-Induced Diastereomers for Chiral Separation, Phys. Rev. Lett. **123**, 243202 (2019).

[49] H. Schmiedt, S. Schlemmer, S. N. Yurchenko, A. Yachmenev, and P. Jensen, A semi-classical approach to the calculation of highly excited rotational energies for asymmetric-top molecules, Phys. Chem. Chem. Phys. **19**, 1847 (2017).

[50] E. Gershnabel and I. Sh. Averbukh, Electric deflection of rotating molecules, J. Chem. Phys. **134**, 054304 (2011).

[51] E. Gershnabel and I. Sh. Averbukh, Deflection of rotating symmetric top molecules by inhomogeneous fields, J. Chem. Phys. **135**, 084307 (2011).

[52] Y.-P. Chang, D. A. Horke, S. Trippel, and J. Küpper, Spatially-controlled complex molecules and their applications, Int. Rev. Phys. Chem. **34**, 557 (2015).